

Multi-Pair D2D Communications Aided by An Active RIS over Spatially Correlated Channels with Phase Noise

Zhangjie Peng, Xue Liu, Cunhua Pan, *Member, IEEE*, Li Li, and Jiangzhou Wang, *Fellow, IEEE*

Abstract—This paper investigates a multi-pair device-to-device (D2D) communication system aided by an active reconfigurable intelligent surface (RIS) with phase noise and direct link. The approximate closed-form expression of the ergodic sum rate is derived over spatially correlated Rician fading channels with statistical channel state information (CSI). When the Rician factors go to infinity, the asymptotic expressions of the ergodic sum rates are presented to give insights in poor scattering environment. The power scaling law for the special case of a single D2D pair is presented without phase noise under uncorrelated Rician fading condition. Then, to solve the ergodic sum rate maximization problem, a method based on genetic algorithm (GA) is proposed for joint power control and discrete phase shifts optimization. Simulation results verify the accuracy of our derivations, and also show that the active RIS outperforms the passive RIS.

Index Terms—Reconfigurable intelligent surface (RIS), active RIS, device-to-device (D2D) communication, ergodic sum rate, phase noise, spatial correlation, power control.

I. INTRODUCTION

Recently, reconfigurable intelligent surface (RIS) has emerged as a brand new communication paradigm to reconfigure the radio propagation environment in a desired manner [1]. To be specific, RIS is an array of reflecting elements, each of which can independently induce a phase shift on the incident signals. By carefully tuning the phase shifts, RIS can be utilized for reducing the sum power [2] and enhancing the system sum rate [3]. The RIS also possesses the advantages of small size, light weight, convenient deployment and low cost.

On the other hand, device-to-device (D2D) technology is also regarded as a promising solution to alleviate the capacity demand of local transmission. The integration of RIS in D2D communications has sparked extensive research efforts [4], [5]. In [4], the power allocation scheme was presented and an RIS was deployed to improve the system sum rate by eliminating the interference of D2D communications. In [5], the energy efficiency was maximized through jointly

optimizing the power allocation and the phase shifts in D2D communication network.

However, the RIS considered in [1]–[5] is passive, which can only reflect the incident signal without any signal processing operations. The performance gain brought by the passive RIS is limited due to the “multiplicative fading” effect with strong direct links between the base station and the users [6]. To address this issue, active RIS has been proposed, which can amplify the incident signals in the electromagnetic level and adjust the phase shifts, concurrently [7]. Different from amplify-and-forward relays, the active RIS operates in full-duplex mode and is equipped with low-power reflection-type amplifiers instead of power-hungry radio frequency chains [8]. The active RIS inherits the advantages of the passive RIS, while its superiorities have been demonstrated in [9]. However, the contributions in [6]–[9] were based on the assumption of the availability of instantaneous channel state information (CSI), which results in high channel estimation overhead. To tackle this issue, the authors in [10]–[13] designed the RIS phase shifts exploiting statistical CSI, which varies much slower and can relax the necessity for configuring the RIS frequently. Besides, the impact of spatial correlation is non-negligible since the reflecting elements are located close to each other due to the small size of the RIS. The performance of RIS-aided cell-free massive multiple-input multiple-output (MIMO) system was analyzed under the presence of spatial correlation [10]. The ergodic sum rate was studied and maximized in the RIS-aided MIMO multiple-access channel system over spatially correlated Rician fading with statistical CSI [11]. The outage probability in RIS-aided communication system was investigated in [12] and the impact of the Von Mises phase errors of the reflecting elements was further studied in [13].

In this paper, we investigate a multi-pair D2D communication system aided by an active RIS over spatially correlated Rician fading channels, where only statistical CSI is available to reduce the channel estimation overhead. It is noted that our work differs from [14] where the RIS was used as a receiver. The contributions of this paper are summarized as follows: 1) The approximate closed-form expression of the ergodic sum rate is derived; 2) We propose a method based on genetic algorithm (GA) to maximize the ergodic sum rate through joint power control and discrete phase shifts optimization; 3) Simulation results validate the accuracy of our derivations and the superiority of the active RIS over the passive RIS.

II. SYSTEM MODEL

Consider a D2D overlaying communication system as depicted in Fig. 1, which serves K pairs of single antenna users. The base station acts as a controller, which not only allocates the power and the spectrum resources for the D2D user-pairs, collects all the statistical CSI estimated by the devices

This work was supported in part by the Natural Science Foundation of Shanghai under Grant 22ZR1445600, in part by the open research fund of National Mobile Communications Research Laboratory, Southeast University under Grant 2018D14, and in part by the National Natural Science Foundation of China under Grant 61701307. (*Corresponding authors: Cunhua Pan and Xue Liu.*)

Zhangjie Peng is with the College of Information, Mechanical and Electrical Engineering, Shanghai Normal University, Shanghai 200234, China, also with the National Mobile Communications Research Laboratory, Southeast University, Nanjing 210096, China, and also with the Shanghai Engineering Research Center of Intelligent Education and Bigdata, Shanghai Normal University, Shanghai 200234, China (e-mail: pengzhangjie@shnu.edu.cn).

X. Liu and L. Li are with the College of Information, Mechanical and Electrical Engineering, Shanghai Normal University, Shanghai 200234, China (e-mail: 1000494962@smail.shnu.edu.cn; lilyxuan@shnu.edu.cn).

C. Pan is with the National Mobile Communications Research Laboratory, Southeast University, Nanjing 210096, China. (e-mail: cpan@seu.edu.cn).

J. Wang is with the School of Engineering, University of Kent, CT2 7NT Canterbury, U.K. (e-mail: j.z.wang@kent.ac.uk).

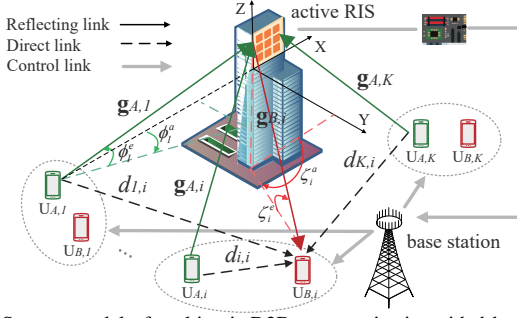


Fig. 1. System model of multi-pair D2D communication aided by an active RIS.

but also performs the power control and the optimization of RIS phase shifts. The active RIS with $N = N_H N_V$ reflecting elements is deployed to further enhance the communication performance. The phase shift matrix is expressed as $\Theta = \text{diag}(e^{j\theta_1}, \dots, e^{j\theta_n}, \dots, e^{j\theta_N}) \in \mathbb{C}^{N \times N}$, where $n = 1, \dots, N$. The phase noise is considered due to the hardware limit of the active RIS. The phase noise matrix is denoted as $\Phi = \text{diag}(e^{j\tilde{\theta}_1}, \dots, e^{j\tilde{\theta}_n}, \dots, e^{j\tilde{\theta}_N})$ and $\tilde{\theta}_n$ follows the circular normal distribution with zero mean and concentration parameter $\kappa_{\tilde{\theta}}$ [15]. The amplification factor matrix is $\Lambda = \text{diag}(\eta_1, \dots, \eta_n, \dots, \eta_N)$. The amplification noise is $\mathbf{n}_F \sim \mathcal{CN}(\mathbf{0}, \sigma_F^2 \mathbf{I})$ and $\mathbf{n}_F \in \mathbb{C}^{N \times 1}$.

We denote the i -th D2D user-pair as $U_{A,i}$ and $U_{B,i}$ for $i = 1, \dots, K$. The transmit power of $U_{A,i}$ is P_i , and $s_{A,i}$ stands for the information symbol with unit power.

The direct channel link between $U_{A,i}$ and $U_{B,j}$ is denoted as $h_{i,j}$, which is assumed to follow the Rician fading in the short communication distance, i.e., $h_{i,j} \sim \mathcal{CN}(\bar{h}_{i,j}, \sigma_{i,j}^2/(1 + \gamma_{i,j}))$ where $\bar{h}_{i,j} = \sigma_{i,j} \sqrt{\gamma_{i,j}/(1 + \gamma_{i,j})}$. $\bar{h}_{i,j}$ is the line-of-sight (LoS) component, $\sigma_{i,j}^2$ is the large-scale fading coefficient and $\gamma_{i,j}$ is the Rician factor. The reflecting channels $U_{A,i} \rightarrow \text{RIS}$ and $\text{RIS} \rightarrow U_{B,i}$ are assumed to follow the spatially correlated Rician fading since the active RIS is usually deployed in high altitude with LoS components [16]:

$$\mathbf{g}_{A,i} = \sqrt{\alpha_i \gamma_{A,i} / (1 + \gamma_{A,i})} \bar{\mathbf{g}}_{A,i} + \sqrt{\alpha_i / (1 + \gamma_{A,i})} \tilde{\mathbf{g}}_{A,i}, \quad (1)$$

$$\mathbf{g}_{B,i} = \sqrt{\beta_i \gamma_{B,i} / (1 + \gamma_{B,i})} \bar{\mathbf{g}}_{B,i} + \sqrt{\beta_i / (1 + \gamma_{B,i})} \tilde{\mathbf{g}}_{B,i}, \quad (2)$$

where $\mathbf{g}_{A,i}, \mathbf{g}_{B,i} \in \mathbb{C}^{N \times 1}$. α_i and β_i denote the large-scale fading coefficients. $\gamma_{A,i}$ and $\gamma_{B,i}$ are the Rician factors. $\bar{\mathbf{g}}_{A,i}$ and $\bar{\mathbf{g}}_{B,i}$ are non-line-of-sight (NLoS) components, which are distributed as $\bar{\mathbf{g}}_{A,i} \sim \mathcal{CN}(\mathbf{0}, \mathbf{R})$ and $\bar{\mathbf{g}}_{B,i} \sim \mathcal{CN}(\mathbf{0}, \mathbf{R})$, respectively. \mathbf{R} stands for the normalized spatial correlation matrix under the isotropic scattering model, whose (p, q) -th element $[\mathbf{R}]_{p,q}$ is [16, Eq. (10)].

$$r_{p,q} = \text{sinc}\left(2\sqrt{(h(p) - h(q))^2 d_H^2 + (v(p) - v(q))^2 d_V^2} / \lambda\right), \quad (3)$$

where $h(p) = \text{mod}(p - 1, N_H)$ and $v(p) = \lfloor (p - 1) / N_H \rfloor$. d_H and d_V are the horizontal and vertical element-spacing, λ is the wavelength and we set $d_H = d_V = \frac{1}{4}\lambda$. $\bar{\mathbf{g}}_{A,i}$ and $\bar{\mathbf{g}}_{B,i}$ represent the LoS components under the uniform planar array (UPA) model, which are respectively written as

$$\bar{\mathbf{g}}_{A,i} = \begin{bmatrix} 1, \dots, e^{j\frac{2\pi}{\lambda}(h(n)d_H \sin \phi_i^a \cos \phi_i^e + v(n)d_V \sin \phi_i^e)}, \dots \end{bmatrix}^T, \quad (4)$$

$$\bar{\mathbf{g}}_{B,i} = \begin{bmatrix} 1, \dots, e^{j\frac{2\pi}{\lambda}(h(n)d_H \sin \zeta_i^a \cos \zeta_i^e + v(n)d_V \sin \zeta_i^e)}, \dots \end{bmatrix}^T, \quad (5)$$

where ϕ_i^a and ϕ_i^e denote the azimuth and elevation angles of

arrival (AoA), ζ_i^a and ζ_i^e denote the azimuth and elevation angles of departure (AoD). The amplification power of the active RIS is given by

$$\sum_{i=1}^K P_i \mathbb{E} \left\{ \|\Lambda \Theta \Phi \mathbf{g}_{A,i}\|^2 \right\} + \mathbb{E} \left\{ \|\Lambda \Theta \Phi \mathbf{n}_F\|^2 \right\} = P_R, \quad (6)$$

where the expectation is taken over the NLoS components in the channels. The total power consumption of the active RIS aided system is

$$P_T = \sum_{i=1}^K P_i + \varepsilon^{-1} P_R + N(P_{DC} + P_{SW}), \quad (7)$$

where ε is the amplifier efficiency, P_{DC} and P_{SW} represent the direct current biasing power consumption and the power consumption of the switch and control circuit at each reflecting element [7]. In addition, the signal received at the j -th D2D receiver is given by

$$y_j = \underbrace{\sqrt{P_j} g_{j,j} s_{A,j}}_{\text{desired signal}} + \underbrace{\sum_{i \neq j}^K \sqrt{P_i} g_{i,j} s_{A,i}}_{\text{inter-pair interference}} + \underbrace{\mathbf{g}_{B,j}^T \Lambda \Theta \Phi \mathbf{n}_F}_{\text{dynamic noise}} + \underbrace{n_j}_{\text{static noise}}, \quad (8)$$

where $g_{i,j} = \mathbf{g}_{B,j}^T \Lambda \Theta \Phi \mathbf{g}_{A,i} + h_{i,j}$ and $n_j \sim \mathcal{CN}(0, \sigma_j^2)$.

The signal-to-interference plus noise ratio (SINR) at $U_{B,j}$ is

$$\gamma_j = \frac{P_j |g_{j,j}|^2}{\sum_{i \neq j}^K P_i |g_{i,j}|^2 + \|\mathbf{g}_{B,j}^T \Lambda \Theta \Phi\|^2 \sigma_F^2 + \sigma_j^2}. \quad (9)$$

Then, the ergodic rate is expressed as

$$R_j = \mathbb{E} \left\{ \log_2(1 + \gamma_j) \right\}, \quad (10)$$

and the ergodic sum rate is $R = \sum_{j=1}^K R_j$.

III. ERGODIC SUM RATE ANALYSIS

In this section, the approximate closed-form expression of the ergodic sum rate is derived with statistical CSI, which contains the spatial correlation, the location and angle information of the transceivers. First, we assume that the amplification factor of each element is the same, i.e., $\eta_n = \eta$, which is derived below.

Lemma 1. The amplification factor for each element on the active RIS is given by

$$\eta = \sqrt{P_R} / \sqrt{N \left(\sum_{i=1}^K P_i \alpha_i + \sigma_F^2 \right)}. \quad (11)$$

Proof. With $\mathbb{E} \{ \Phi^H \Theta^H \Lambda^H \Lambda \Theta \Phi \} = \eta^2 \mathbf{I}_{N \times N}$, we can derive $\mathbb{E} \{ \|\Lambda \Theta \Phi \mathbf{g}_{A,i}\|^2 \} = \frac{\alpha_i \eta^2}{1 + \gamma_{A,i}} (\gamma_{A,i} \mathbb{E} \{ \bar{\mathbf{g}}_{A,i} \bar{\mathbf{g}}_{A,i}^H \} + \mathbb{E} \{ \tilde{\mathbf{g}}_{A,i} \tilde{\mathbf{g}}_{A,i}^H \}) = \frac{\alpha_i \eta^2}{1 + \gamma_{A,i}} (\gamma_{A,i} N + N) = \eta^2 N \alpha_i$. Similarly, we have $\mathbb{E} \{ \|\Lambda \Theta \Phi \mathbf{n}_F\|^2 \} = \eta^2 N \sigma_F^2$. Substituting these results into (6) yields $\eta^2 N (\sum_{i=1}^K P_i \alpha_i + \sigma_F^2) = P_R$. \square

Based on Lemma 1, the approximation of the ergodic rate is given in the following theorem.

Theorem 1. For the considered multi-pair D2D communication system assisted by an active RIS over spatially correlated channels with phase noise, the closed-form expression of the approximate ergodic rate of $U_{B,j}$ is given by $R_j \approx \tilde{R}_j$, where

$$\tilde{R}_j = \log_2 \left(1 + \frac{P_j (\eta^2 \Omega_{j,j} + 2\eta c_{j,j} \Upsilon_{j,j} + \sigma_{j,j}^2)}{\sum_{i \neq j}^K P_i (\eta^2 \Omega_{i,j} + 2\eta c_{i,j} \Upsilon_{i,j} + \sigma_{i,j}^2) + \eta^2 N \beta_j \sigma_F^2 + \sigma_j^2} \right), \quad (12)$$

in which $\Omega_{i,j} = \alpha_i \beta_j N + \tau_{i,j}(\gamma_{A,i} \gamma_{B,j} \Gamma_{i,j} + \gamma_{B,j} L_{\zeta_i^a, \zeta_i^e} + \gamma_{A,i} L_{\phi_i^a, \phi_i^e} + L_0)$, $\tau_{i,j} = \frac{\alpha_i \beta_j}{(1 + \gamma_{A,i})(1 + \gamma_{B,j})}$, $\Gamma_{i,j}$, $L_{x,y}$, L_0 and $\Upsilon_{i,j}$ are given in (23), (25), (27) and (30) in Appendix A.

Proof. See Appendix A. \square

Remark 1. 1) By setting the values of η and σ_F^2 in (12) with $\eta = 1$ and $\sigma_F^2 = 0$, the ergodic rate in the passive RIS case is written as

$$\tilde{R}_j^{pas} = \log_2 \left(1 + \frac{P'_j (\Omega_{j,j} + 2c_{j,j} \Upsilon_{j,j} + \sigma_{j,j}^2)}{\sum_{i \neq j}^K P'_i (\Omega_{i,j} + 2c_{i,j} \Upsilon_{i,j} + \sigma_{i,j}^2) + \sigma_j^2} \right). \quad (13)$$

2) Furthermore, when $\Omega_{i,j} = \Omega_{j,j} = 0$ and $\Upsilon_{i,j} = \Upsilon_{j,j} = 0$ for any i and j , we derive the ergodic rate in the case without RIS, which is given by

$$\tilde{R}_j^{noRIS} = \log_2 \left(1 + \frac{P''_j \sigma_{j,j}^2}{\sum_{i \neq j}^K P''_i \sigma_{i,j}^2 + \sigma_j^2} \right). \quad (14)$$

The total power consumption in the passive RIS case and the case without RIS are $P_T^{pas} = \sum_{i=1}^K P'_i + NP_{SW}$ and $P_T^{noRIS} = \sum_{i=1}^K P''_i$, respectively. For fairness, we assume $P_T = P_T^{pas} = P_T^{noRIS} = P$. Besides, when the RIS hardware is ideal, i.e., $\Phi = \mathbf{I}_{N \times N}$, the ergodic rates without phase noise are rewritten by substituting $\kappa = 1$ into (12) and (13).

Corollary 1. When the Rician factors go to infinity, i.e., $\gamma_{A,i} = \gamma_{B,i} = \gamma_{A,j} = \gamma_{B,j} = \gamma_{i,j} = \gamma_{j,j} \rightarrow \infty$ for any i and j , the ergodic rates \tilde{R}_j in (12) and \tilde{R}_j^{pas} in (13) converge to

$$\tilde{R}_j \rightarrow \bar{R}_j, \tilde{R}_j^{pas} \rightarrow \bar{R}_j^{pas}, \quad (15)$$

where \bar{R}_j and \bar{R}_j^{pas} are given by (16) and (17), respectively.

Corollary 1 means that when the communication environment has limited scatters, the ergodic rates converge to fixed values depending on the phase shifts.

Corollary 2. If the total power consumption $P \rightarrow \infty$ (i.e., $P_R \rightarrow \infty$, $P_i \approx P'_i \approx P_j \approx P'_j \rightarrow \infty$ for any i and j) and the direct links are non-exist due to the blockage, we can derive that $\tilde{R}_j \rightarrow \bar{R}_j$ and $\tilde{R}_j^{pas} \rightarrow \bar{R}_j^{pas}$, where

$$\bar{R}_j = \log_2 \left(1 + \frac{\Omega_{j,j}}{\sum_{i \neq j}^K \Omega_{i,j}} \right). \quad (18)$$

Corollary 2 shows that the ergodic rate of the active RIS aided system with high transmit power converges to the same value as the passive RIS counterpart. This is because the dynamic noise caused by active RIS and the static noise are negligible, and the power of both the desired signal and the multi-pair interferences increase by the same factor of η^2 . In other words, the ergodic sum rate in passive RIS case is close to the active counterpart at high power consumption.

Remark 2. If $\mathbf{R} = \mathbf{I}_{N \times N}$, the reflecting links are simplified to uncorrelated Rician fading channel. Then, we consider a special case that there is only one user-pair ($U_{A,i}$ and $U_{B,i}$) and the direct link is blocked, the ergodic rate becomes $\tilde{R}_1 = \log_2 \left(1 + \frac{P_i P_R \Omega_{i,i}^*}{N P_R \beta_i \sigma_F^2 + N (P_i \alpha_i + \sigma_F^2) \sigma_i^2} \right)$ where $\Omega_{i,i}^* = \alpha_i \beta_i N + \tau_{i,i} \gamma_{A,i} \gamma_{B,i} \Gamma_{i,i}$. Assuming that the hardware

Algorithm 1 GA-based method

Input: the population size N_{po} , the number of parents N_{pa} , the number of mutated chromosomes N_{mu} , the maximum iteration number N_i and the termination fitness value f .

Output: the elite $e_t = [p_t, \theta_t]$ of each generation.

Initialize: the first generation e_s for $s = 1, \dots, N_{po}$,

- 1: **for** $t = 1$ to N_i **do**
- 2: Calculate the fitness value $f(e_s) = \frac{1}{\bar{R}(p_s, \theta_s)}$;
- 3: Note down e_t with the minimum fitness value;
- 4: **if** $f(e_t) > f$ **then**
- 5: Applying roulette wheel selection on the individuals (except e_t) to get N_{pa} parent chromosomes;
- 6: Cut off the parent chromosomes at a random place c for $c = 1, \dots, K + N$;
- 7: Hybridize them to produce children chromosomes;
- 8: Chose N_{mu} chromosome and mutated places n'_1, n'_2 at random for $n'_1 = 1, \dots, K$ and $n'_2 = 1, \dots, N$;
- 9: Update $p_{n'_1}$ with a random value subject to (19b);
- 10: Update $\theta_{n'_2}$ with a random value subject to (19c);
- 11: **end if**
- 12: **end for**

of the active RIS is ideal, if the transmit power P_i is scaled down by $\frac{1}{N}$, i.e. $P_i = \frac{E_u}{N}$ for a fixed E_u , we have $\tilde{R}_1 \rightarrow \log_2 \left(1 + \frac{E_u P_R \tau_{i,i} \gamma_{A,i} \gamma_{B,i}}{P_R \beta_i \sigma_F^2 + \sigma_F^2 \sigma_i^2} \right)$ as $N \rightarrow \infty$.

Proof. See Appendix B. \square

IV. POWER CONTROL AND PHASE SHIFTS OPTIMIZATION

In this section, we propose a GA-based method to jointly optimize the transmit power and the phase shifts to maximize the ergodic sum rate. Due to the hardware limit, the discrete phase shift design is considered and the optimization problem is formulated as follows:

$$\max_{\mathbf{p}, \boldsymbol{\theta}} \tilde{R} = \sum_{j=1}^K \tilde{R}_j \quad (19a)$$

$$\text{s.t. } 0 < p_i \leq p_{max}, \forall i = 1, \dots, K, \quad (19b)$$

$$\theta_n \in \{0, 2\pi/2^B, \dots, (2^B - 1)2\pi/2^B\}, \forall n = 1, \dots, N, \quad (19c)$$

where $\mathbf{p} = [p_1, p_2, \dots, p_K]$, $\boldsymbol{\theta} = [\theta_1, \theta_2, \dots, \theta_N]$ and B is the number of bits for controlling the phase shifts.

Note that GA is a globally search method inspired by imitating the biological evolution, which can automatically accumulate knowledge about the search space, and adaptively control the search process to obtain the optimal solution. The details of our proposed GA-based method are given in Algorithm 1.

V. NUMERICAL RESULTS

In this section, we provide simulation results to demonstrate the correctness of our derivations and evaluate the performance of the proposed algorithm. The RIS is deployed at (30 m, 0 m,

$$\bar{R}_j = \log_2 \left(1 + \frac{P_j (\alpha_j \beta_j \eta^2 (N + \Gamma_{j,j}) + 2\eta \kappa \sigma_{j,j} \sqrt{\alpha_j \beta_j} \Upsilon_{j,j} + \sigma_{j,j}^2)}{\sum_{i \neq j}^K P_i (\alpha_i \beta_j \eta^2 (N + \Gamma_{i,j}) + 2\eta \kappa \sigma_{i,j} \sqrt{\alpha_i \beta_j} \Upsilon_{i,j} + \sigma_{i,j}^2) + \eta^2 N \beta_j \sigma_F^2 + \sigma_j^2} \right), \quad (16)$$

$$\bar{R}_j^{pas} = \log_2 \left(1 + \frac{P_j (\alpha_j \beta_j (N + \Gamma_{j,j}) + 2\kappa \sigma_{j,j} \sqrt{\alpha_j \beta_j} \Upsilon_{j,j} + \sigma_{j,j}^2)}{\sum_{i \neq j}^K P_i (\alpha_i \beta_j (N + \Gamma_{i,j}) + 2\kappa \sigma_{i,j} \sqrt{\alpha_i \beta_j} \Upsilon_{i,j} + \sigma_{i,j}^2) + \sigma_j^2} \right). \quad (17)$$

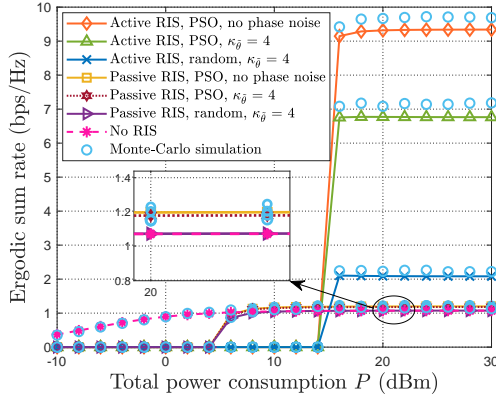


Fig. 2. The ergodic sum rate versus the total power consumption.

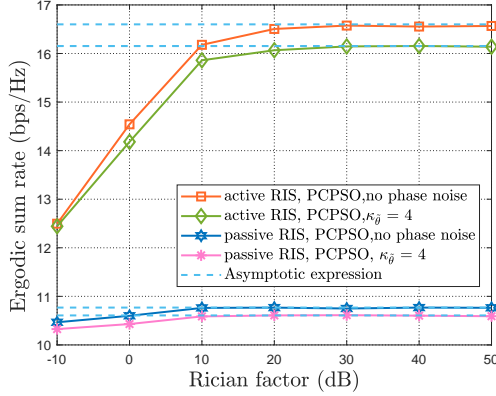


Fig. 3. The ergodic sum rate versus the Rician factor.

8 m) with $N = 32$ elements. The number of D2D user-pairs are set to $K = 6$, which are distributed in a rectangular plane with four points (0 m, 0 m, 1.6 m), (60 m, 0 m, 1.6 m), (0 m, 25 m, 1.6 m) and (60 m, 25 m, 1.6 m). The large-scale fading coefficients are $PL = -30 - 10\chi \log_{10}(d)$ dB, where χ is the path-loss exponent, and d is the distance between the D2D users (or the D2D user and the RIS) in meters. We set $\chi_d = 3.8$ for the direct links and $\chi_r = 2.2$ for the reflecting links. The AoA and AoD of all channels are randomly generated from $[0, 2\pi)$. The Rician factors are set to 10 dB. Unless stated otherwise, we set $P = 30$ dBm, $B = 3$, $\kappa_{\bar{\theta}} = 4$, $\sigma_F^2 = -70$ dBm, $\sigma_j^2 = -80$ dBm [8], $P_{DC} = -5$ dBm, $P_{SW} = -10$ dBm, $\varepsilon = 0.8$ [7]. Note that the curves marked “PCPSO” represent joint power control and phase shifts optimization while the curves marked “PSO” represent optimizing the phase shifts with equal power allocation.

Fig. 2 depicts the ergodic sum rate versus P with both random and optimized phase shifts in different cases. When P is too small to support hardware power consumption, the ergodic rate is set to zero, i.e., $\bar{R}_j = 0$ when $P \leq N(P_{DC} + P_{SW})$ and $\bar{R}_j^{pas} = 0$ when $P \leq NP_{SW}$. It can be observed that the closed-form expression in (12) matches well with the Monte-Carlo simulation in (10), which validates the accuracy of our derived results. We observe that the active RIS outperforms the passive RIS while the passive RIS achieves negligible performance gain compared with the case without RIS. As expected, the ergodic sum rates without phase noise are higher. In addition, the proposed GA-based method shows its effectiveness on rate improvement compared with the random phase shifts, which demonstrates the importance of designing the phase shifts. It also indicates that the active RIS

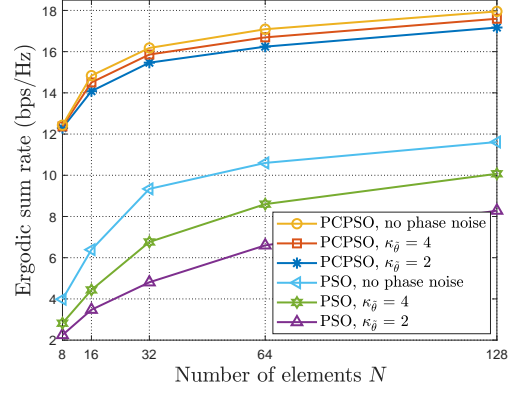


Fig. 4. The ergodic sum rate versus the number of elements N .

can overcome the “multiplicative fading” effect and achieve noticeable performance gains compared with the passive RIS.

In Fig. 3, the curves marked as “Asymptotic expression” are obtained by Corollary 1. The figure shows that the ergodic sum rates notably increase as Rician factors increase at the beginning and converge to constants when the LoS components are large. In other words, the ergodic sum rates are relatively higher in poor scattering environment, which is consistent with the conclusion in [17]. Hence, the RIS should be deployed in the places with poor scatters.

It can be seen from Fig. 4 that the ergodic sum rates increase with the number of reflecting elements N in the active RIS aided system. Even a few elements may improve the ergodic sum rates significantly. In addition, the ergodic sum rates decrease with the decrease of the phase noise parameter $\kappa_{\bar{\theta}}$. Increasing the number of reflecting elements achieves limited performance gain when N is large. However, the power control can achieve potential gains with the increase of N , and is shown to be an effective way on performance improvement compared with equal power allocation. Therefore, deploying an active RIS with a small number of reflecting elements is sufficient to achieve significant performance gains.

VI. CONCLUSION

This letter investigated the system performance for a multi-pair D2D communication system aided by an active RIS over spatially correlated channels with phase noise and direct link. The approximate closed-form expression of the ergodic sum rate was derived and analyzed under different channel conditions. The impact of the phase noise on the ergodic sum rate was also discussed. The proposed GA-based method was effective for ergodic sum rate maximization. The simulation results showed that the active RIS outperforms the passive RIS.

APPENDIX A

By using [18, Lemma 1], the ergodic rate can be approximated by

$$R_j \approx \log_2 \left(1 + \frac{P_j \mathbb{E}\{|g_{j,j}|^2\}}{\sum_{i \neq j}^K P_i \mathbb{E}\{|g_{i,j}|^2\} + \mathbb{E}\left\{\left\|\mathbf{g}_{B,j}^T \mathbf{\Lambda} \mathbf{\Theta} \mathbf{\Phi}\right\|^2\right\} \sigma_F^2 + \sigma_j^2} \right). \quad (20)$$

Since $\tilde{\mathbf{g}}_{A,i}$, $\tilde{\mathbf{g}}_{B,i}$ and $h_{i,j}$ are independent of each other, we have $\mathbb{E}\{|g_{i,j}|^2\} = \mathbb{E}\{|\mathbf{g}_{B,j}^T \mathbf{\Lambda} \mathbf{\Theta} \Phi \mathbf{g}_{A,i}|^2\} + \sigma_{i,j}^2 + 2\mathbb{E}\{\text{Re}\{\mathbf{g}_{B,j}^T \mathbf{\Lambda} \mathbf{\Theta} \Phi \mathbf{g}_{A,i} h_{i,j}^*\}\}$. First, we derive that

$$\begin{aligned} \mathbb{E}\{|\mathbf{g}_{B,j}^T \mathbf{\Lambda} \mathbf{\Theta} \Phi \mathbf{g}_{A,i}|^2\} &= \mathbb{E}\{\mathbf{g}_{B,j}^T \mathbf{\Lambda} \mathbf{\Theta} \Phi \mathbf{g}_{A,i} \mathbf{g}_{A,i}^H \Phi^H \mathbf{\Theta}^H \mathbf{\Lambda}^H \mathbf{g}_{B,j}^*\} \\ &\stackrel{(a)}{=} \tau_{i,j}(\gamma_{A,i} \gamma_{B,j} \mathbb{E}\{\mathbf{g}_{B,j}^T \mathbf{\Lambda} \mathbf{\Theta} \Phi \tilde{\mathbf{g}}_{A,i} \tilde{\mathbf{g}}_{A,i}^H \Phi^H \mathbf{\Theta}^H \mathbf{\Lambda}^H \tilde{\mathbf{g}}_{B,j}^*\} \\ &\quad + \gamma_{B,j} \mathbb{E}\{\mathbf{g}_{B,j}^T \mathbf{\Lambda} \mathbf{\Theta} \Phi \tilde{\mathbf{g}}_{A,i} \tilde{\mathbf{g}}_{A,i}^H \Phi^H \mathbf{\Theta}^H \mathbf{\Lambda}^H \tilde{\mathbf{g}}_{B,j}^*\} \\ &\quad + \gamma_{A,i} \mathbb{E}\{\tilde{\mathbf{g}}_{B,j}^T \mathbf{\Lambda} \mathbf{\Theta} \Phi \tilde{\mathbf{g}}_{A,i} \tilde{\mathbf{g}}_{A,i}^H \Phi^H \mathbf{\Theta}^H \mathbf{\Lambda}^H \tilde{\mathbf{g}}_{B,j}^*\} \\ &\quad + \mathbb{E}\{\tilde{\mathbf{g}}_{B,j}^T \mathbf{\Lambda} \mathbf{\Theta} \Phi \tilde{\mathbf{g}}_{A,i} \tilde{\mathbf{g}}_{A,i}^H \Phi^H \mathbf{\Theta}^H \mathbf{\Lambda}^H \tilde{\mathbf{g}}_{B,j}^*\}), \end{aligned} \quad (21)$$

where (a) is derived by removing zero terms. Then, we can obtain the following result according to the Euler's formula.

$$\begin{aligned} &\mathbb{E}\{\mathbf{g}_{B,j}^T \mathbf{\Lambda} \mathbf{\Theta} \Phi \tilde{\mathbf{g}}_{A,i} \tilde{\mathbf{g}}_{A,i}^H \Phi^H \mathbf{\Theta}^H \mathbf{\Lambda}^H \tilde{\mathbf{g}}_{B,j}^*\} \\ &= \eta^2 \mathbb{E}\left\{\sum_{n=1}^N e^{j(\theta_n + \bar{\theta}_n)} [\tilde{\mathbf{g}}_{B,j}]_n [\tilde{\mathbf{g}}_{A,i}]_n\right\}^2 = \eta^2 (N + \Gamma_{i,j}), \end{aligned} \quad (22)$$

where

$$\Gamma_{i,j} = 2\kappa^2 \sum_{1 \leq q < p \leq N} \cos(\theta_p - \theta_q + (2\pi/\lambda)(\bar{s}_{p,q}^{i,j} + \bar{t}_{p,q}^{i,j})), \quad (23)$$

$\bar{s}_{p,q}^{i,j} = (h(p) - h(q)) d_H(\sin \phi_i^a \cos \phi_i^e + \sin \zeta_j^a \cos \zeta_j^e)$ and $\bar{t}_{p,q}^{i,j} = (v(p) - v(q)) d_V(\sin \phi_i^e + \sin \zeta_j^e)$. Here, $\kappa = \frac{I_1(\kappa_{\bar{\theta}})}{I_0(\kappa_{\bar{\theta}})}$, and $I_p(\kappa_{\bar{\theta}})$ is the modified Bessel function of the first kind and order p [15]. Next, applying $\mathbb{E}\{\Phi \mathbf{R} \Phi^H\} = \mathbb{E}\{\Phi^H \mathbf{R} \Phi\} = \kappa^2 \mathbf{R} + (1 - \kappa^2) \mathbf{I}_{N \times N}$, we can derive that

$$\begin{aligned} &\mathbb{E}\{\mathbf{g}_{B,j}^T \mathbf{\Lambda} \mathbf{\Theta} \Phi \tilde{\mathbf{g}}_{A,i} \tilde{\mathbf{g}}_{A,i}^H \Phi^H \mathbf{\Theta}^H \mathbf{\Lambda}^H \tilde{\mathbf{g}}_{B,j}^*\} \\ &= \eta^2 \mathbb{E}\{\mathbf{g}_{B,j}^T \mathbf{\Theta} \Phi \mathbb{E}\{\tilde{\mathbf{g}}_{A,i} \tilde{\mathbf{g}}_{A,i}^H\} \Phi^H \mathbf{\Theta}^H \tilde{\mathbf{g}}_{B,j}^*\} \\ &= \eta^2 \mathbb{E}\{\mathbf{g}_{B,j}^T \mathbf{\Theta} \mathbb{E}\{\Phi \mathbf{R} \Phi^H\} \mathbf{\Theta}^H \tilde{\mathbf{g}}_{B,j}^*\} \\ &= \eta^2 (\kappa^2 \mathbb{E}\{\mathbf{g}_{B,j}^T \mathbf{\Theta} \mathbf{R} \mathbf{\Theta}^H \tilde{\mathbf{g}}_{B,j}^*\} + (1 - \kappa^2) \mathbb{E}\{\mathbf{g}_{B,j}^T \tilde{\mathbf{g}}_{B,j}^*\}) \\ &= \eta^2 (\kappa^2 N + L_{\zeta_j^a, \zeta_j^e} + (1 - \kappa^2)N) = \eta^2 (N + L_{\zeta_j^a, \zeta_j^e}), \end{aligned} \quad (24)$$

where

$$L_{x,y} = 2\kappa^2 \sum_{1 \leq q < p \leq N} r_{p,q} \cos(\theta_p - \theta_q + (2\pi/\lambda)(s_{p,q}^{x,y} + t_{p,q}^{x,y})). \quad (25)$$

$r_{p,q}$ is given by (3), $s_{p,q}^{x,y} = (h(p) - h(q)) d_H \sin x \cos y$ and $t_{p,q}^{x,y} = (v(p) - v(q)) d_V \sin y$. Similarly, we have

$$\begin{aligned} &\mathbb{E}\{\mathbf{g}_{B,j}^T \mathbf{\Lambda} \mathbf{\Theta} \Phi \tilde{\mathbf{g}}_{A,i} \tilde{\mathbf{g}}_{A,i}^H \Phi^H \mathbf{\Theta}^H \mathbf{\Lambda}^H \tilde{\mathbf{g}}_{B,j}^*\} \\ &= \eta^2 \mathbb{E}\{\tilde{\mathbf{g}}_{A,i}^H \Phi^H \mathbf{\Theta}^H \mathbb{E}\{\tilde{\mathbf{g}}_{B,j} \tilde{\mathbf{g}}_{B,j}^T\} \mathbf{\Theta} \Phi \tilde{\mathbf{g}}_{A,i}\} \\ &= \eta^2 (\kappa^2 \mathbb{E}\{\tilde{\mathbf{g}}_{A,i}^H \mathbf{\Theta} \mathbf{R} \mathbf{\Theta}^H \tilde{\mathbf{g}}_{A,i}\} + (1 - \kappa^2) \mathbb{E}\{\tilde{\mathbf{g}}_{A,i}^H \tilde{\mathbf{g}}_{A,i}\}) \\ &= \eta^2 (\kappa^2 N + L_{\phi_i^a, \phi_i^e} + (1 - \kappa^2)N) = \eta^2 (N + L_{\phi_i^a, \phi_i^e}), \end{aligned} \quad (26)$$

$$\begin{aligned} &\mathbb{E}\{\tilde{\mathbf{g}}_{B,j}^T \mathbf{\Lambda} \mathbf{\Theta} \Phi \tilde{\mathbf{g}}_{A,i} \tilde{\mathbf{g}}_{A,i}^H \Phi^H \mathbf{\Theta}^H \mathbf{\Lambda}^H \tilde{\mathbf{g}}_{B,j}^*\} \\ &= \eta^2 (N + 2\kappa^2 \sum_{1 \leq q < p \leq N} r_{p,q}^2 \cos(\theta_p - \theta_q)) \triangleq \eta^2 (N + L_0). \end{aligned} \quad (27)$$

Substituting (22), (24), (26) and (27) into (21), we arrive at

$$\begin{aligned} \mathbb{E}\{|\mathbf{g}_{B,j}^T \mathbf{\Lambda} \mathbf{\Theta} \Phi \mathbf{g}_{A,i}|^2\} &= \eta^2 \tau_{i,j}(\gamma_{A,i} \gamma_{B,j} (N + \Gamma_{i,j}) + \gamma_{A,i} (N \\ &\quad + L_{\phi_i^a, \phi_i^e}) + \gamma_{B,j} (N + L_{\zeta_j^a, \zeta_j^e}) + (N + L_0)) \triangleq \eta^2 \Omega_{i,j}. \end{aligned} \quad (28)$$

Similarly, we have

$$\mathbb{E}\{\|\mathbf{g}_{B,j}^T \mathbf{\Lambda} \mathbf{\Theta} \Phi\|^2\} = \eta^2 N \beta_j. \quad (29)$$

Note that $\mathbb{E}\{e^{j\bar{\theta}_n}\} = \kappa$, we can derive that

$$\begin{aligned} \mathbb{E}\{\text{Re}\{\mathbf{g}_{B,j}^T \mathbf{\Lambda} \mathbf{\Theta} \Phi \mathbf{g}_{A,i} h_{i,j}^*\}\} &= \text{Re}\{\tilde{\mathbf{g}}_{B,j}^T \mathbf{\Lambda} \mathbf{\Theta} \mathbb{E}\{\Phi\} \tilde{\mathbf{g}}_{A,i} \bar{h}_{i,j}\} \\ &= \eta c_{i,j} \sum_{n=1}^N \cos(\theta_n + 2\pi l_{i,j}^n / \lambda) \triangleq \eta c_{i,j} \Upsilon_{i,j}, \end{aligned} \quad (30)$$

where $c_{i,j} = \kappa \sigma_{i,j} \sqrt{\tau_{i,j} \gamma_{A,i} \gamma_{B,j} \gamma_{i,j}} / \sqrt{1 + \gamma_{i,j}}$ and $l_{i,j}^n = h(n)$

$$d_H(\sin \phi_i^a \cos \phi_i^e + \sin \zeta_j^a \cos \zeta_j^e) + v(n) d_V(\sin \phi_i^e + \sin \zeta_j^e).$$

We can substitute (11), (28) - (30) into (20) to complete the proof.

APPENDIX B

From (22), we can infer that

$$N + \tilde{\Gamma}_{i,j} \leq \left(\sum_{n=1}^N |e^{j\theta_n} [\tilde{\mathbf{g}}_{B,j}]_n [\tilde{\mathbf{g}}_{A,i}]_n| \right)^2 = N^2, \quad (31)$$

which indicates that the optimal phase shift of each element on the active RIS with ideal hardware is $\theta_n^{opt} = -\frac{2\pi}{\lambda} (h(n) d_H(\sin \phi_i^a \cos \phi_i^e + \sin \zeta_i^a \cos \zeta_i^e) + v(n) d_V(\sin \phi_i^e + \sin \zeta_i^e)) + C$, where C is an arbitrary constant. Recalling $\Omega_{i,i}^*$ in Remark 2, we have $\Omega_{i,i}^{*,opt} = \tau_{i,i}(\gamma_{A,i} \gamma_{B,i} N^2 + (\gamma_{A,i} + \gamma_{B,i})N + N)$. Substituting $\Omega_{i,i}^*$ with $\Omega_{i,i}^{*,opt}$ into \tilde{R}_1 yields $\tilde{R}_1^{opt} = \log_2 \left(1 + \frac{E_u P_R \tau_{i,i}(\gamma_{A,i} \gamma_{B,i} + \frac{1}{N}(\gamma_{A,i} + \gamma_{B,i}) + \frac{1}{N})}{P_R \beta_i \sigma_F^2 + \frac{E_u}{N} \alpha_i \sigma_i^2 + \sigma_F^2 \sigma_i^2} \right)$. When $N \rightarrow \infty$, we have $\frac{1}{N} \rightarrow 0$ and $R_1 \rightarrow \tilde{R}_1^{opt}$. We arrive at the final result after removing the zero terms.

REFERENCES

- [1] C. Pan *et al.*, "Reconfigurable intelligent surfaces for 6G systems: Principles, applications, and research directions," *IEEE Commun. Mag.*, vol. 59, no. 6, pp. 14–20, Jun. 2021.
- [2] Q. Wu and R. Zhang, "Intelligent reflecting surface enhanced wireless network via joint active and passive beamforming," *IEEE Trans. Wireless Commun.*, vol. 18, no. 11, pp. 5394–5409, Nov. 2019.
- [3] C. Pan *et al.*, "Multicell MIMO communications relying on intelligent reflecting surfaces," *IEEE Trans. Wireless Commun.*, vol. 19, no. 8, pp. 5218–5233, Aug. 2020.
- [4] Y. Chen *et al.*, "Reconfigurable intelligent surface assisted device-to-device communications," *IEEE Trans. Wireless Commun.*, vol. 20, no. 5, pp. 2792–2804, 2021.
- [5] S. Jia, X. Yuan, and Y.-C. Liang, "Reconfigurable intelligent surfaces for energy efficiency in D2D communication network," *IEEE Wireless Commun. Lett.*, vol. 10, no. 3, pp. 683–687, Mar. 2021.
- [6] Z. Zhang *et al.*, "Active RIS vs. Passive RIS: Which will prevail in 6G?" 2021. [Online]. Available: <https://arxiv.org/abs/2103.15154>
- [7] R. Long, Y.-C. Liang, Y. Pei, and E. G. Larsson, "Active reconfigurable intelligent surface-aided wireless communications," *IEEE Trans. Wireless Commun.*, vol. 20, no. 8, pp. 4962–4975, Aug. 2021.
- [8] C. You and R. Zhang, "Wireless communication aided by intelligent reflecting surface: Active or passive?" *IEEE Wireless Commun. Lett.*, vol. 10, no. 12, pp. 2659–2663, Dec. 2021.
- [9] L. Dong, H.-M. Wang, and J. Bai, "Active reconfigurable intelligent surface aided secure transmission," *IEEE Trans. Veh. Technol.*, vol. 71, no. 2, pp. 2181–2186, Feb. 2022.
- [10] T. Van Chien *et al.*, "Reconfigurable intelligent surface-assisted cell-free massive MIMO systems over spatially-correlated channels," *IEEE Trans. Wireless Commun.*, vol. 21, no. 7, pp. 5106–5128, Jul. 2022.
- [11] K. Xu *et al.*, "On the sum-rate of RIS-assisted MIMO multiple-access channels over spatially correlated Rician fading," *IEEE Trans. Commun.*, vol. 69, no. 12, pp. 8228–8241, Dec. 2021.
- [12] P. Xu, W. Niu, G. Chen, Y. Li, and Y. Li, "Performance analysis of RIS-assisted systems with statistical channel state information," *IEEE Trans. Veh. Technol.*, vol. 71, no. 1, pp. 1089–1094, Jan. 2022.
- [13] T. Wang, M.-A. Badiu, G. Chen, and J. P. Coon, "Outage probability analysis of RIS-assisted wireless networks with Von Mises phase errors," *IEEE Wireless Commun. Lett.*, vol. 10, no. 12, pp. 2737–2741, Dec. 2021.
- [14] M. Jung *et al.*, "Performance analysis of large intelligent surfaces (LISs): Asymptotic data rate and channel hardening effects," *IEEE Trans. Wireless Commun.*, vol. 19, no. 3, pp. 2052–2065, Mar. 2020.
- [15] A. Papazafeiropoulos *et al.*, "Intelligent reflecting surface-assisted MU-MISO systems with imperfect hardware: Channel estimation and beamforming design," *IEEE Trans. Wireless Commun.*, vol. 21, no. 3, pp. 2077–2092, Mar. 2022.
- [16] E. Björnson and L. Sanguinetti, "Rayleigh fading modeling and channel hardening for reconfigurable intelligent surfaces," *IEEE Wireless Commun. Lett.*, vol. 10, no. 4, pp. 830–834, Apr. 2021.

- [17] Z. Peng, T. Li, C. Pan, H. Ren, W. Xu, and M. D. Renzo, "Analysis and optimization for RIS-aided multi-pair communications relying on statistical CSI," *IEEE Trans. Veh. Technol.*, p. 3897–3901, Mar. 2021.
- [18] Q. Zhang *et al.*, "Power scaling of uplink massive MIMO systems with arbitrary-rank channel means," *IEEE J. Sel. Topics Signal Process.*, vol. 8, no. 5, pp. 966–981, Oct. 2014.